Solar Energy Materials & Solar Cells 113 (2013) 140–143

Contents lists available at SciVerse ScienceDirect

Solar Energy Materials & Solar Cells

journal homepage: www.elsevier.com/locate/solmat

13.6%-efficient Cu(In,Ga)Se_2 solar cell with absorber fabricated by RF sputtering of $(In,Ga)_2Se_3$ and CuSe targets

X.L. Zhu [a], Y.M. Wang [a,*], Z. Zhou [a], A.M. Li [a], L. Zhang [a], F.Q. Huang [a,b,*]

[a] CAS Key Laboratory of Materials for Energy Conversion, Shanghai Institute of Ceramics, Chinese Academy of Sciences, 1295 Dingxi Road, Shanghai 200050, China
[b] College of Chemistry and Molecular Engineering, Peking University, Beijing 100871, P.R. China

ARTICLE INFO

Article history:
Received 18 February 2012
Received in revised form
18 January 2013
Accepted 1 February 2013
Available online 15 March 2013

Keywords:
Cu(In,Ga)Se_2
Selenide compound target
Sequential sputtering
Thin film solar cells

ABSTRACT

A conversion efficiency of 13.6% has been achieved in Cu(In,Ga)Se_2 (CIGS) thin film solar cell with absorber layer fabricated by sequentially RF sputtering $(In,Ga)_2Se_3$ and CuSe targets and further annealing in Se vapor. The significant improvement, comparing with the efficiency of 10.8% for CIGS solar cell sputtering from a quaternary CIGS target, was attributed to smoother surface, better crystallinity, and more compact structure of the CIGS film. The reaction pathway of $(In,Ga)_2Se_3$/CuSe bilayer was discussed, and such a bilayer design was demonstrated to be energetically favorable to form a better-crystallized CIGS film.

1. Introduction

Cu(In,Ga)Se_2 (CIGS) solar cells have emerged as one of the most promising candidates for high efficiency low-cost thin film solar cells. High-quality CIGS absorbers are usually fabricated by either elemental co-evaporation of individual elements (i.e., Cu, In, Ga and Se) [1] or reactive annealing of metallic precursors (i.e., Cu-In-Ga) under Se or H_2Se ambient [2]. Despite its unquestionable power in preparing high-quality material on small areas, co-evaporation exhibits some problems related to upscaling due to the fact that co-evaporation requires a strict control of evaporation fluxes to achieve the desired film properties.

The selenization of metallic Cu-In-Ga precursors deposited by sputtering from multi-sputtering sources under Se or H_2Se atmospheres may allow easier fabrication of large area CIGS absorbers [2]. However, It was found that In-rich or Cu-rich phases in the sputtered metallic precursors easily resulted in rough morphologies of CIGS layers [3–6]. Another important problem associated with selenized CIGS is the poor adherence of the film to the substrate due to the volume expansion caused by the incorporation of Se into the Cu-In-Ga layers [7,8].

The development and availability of the chalcogenide sputtering targets offers an alternative route to fabricate the CIGS absorbers [9–11], which would not suffer from the above-mentioned lateral non-uniformity, rough morphology and poor adherence to substrate. However, the efficiencies of CIGS solar cells fabricated by the single-target process are relative low (not exceeding 10%) [10].

We have demonstrated a 10.8% efficiency CIGS solar cell, using the CIGS precursor fabricated by RF sputtering from a single quaternary CIGS target, by optimizing the process conditions of Mo layers [12]. However, the average grain size of CIGS obtained by this single-target process was generally small (0.6–0.8 μm), which limited the further improvement of efficiency in a certain extent. In this contribution, we demonstrate the potential of CIGS films by sequentially sputtering two chalcogenide targets of $(In,Ga)_2Se_3$ and CuSe to achieve a higher efficiency.

2. Experimental

The details of the process for CIGS absorber using the CIGS precursor prepared by sputtering from a single quaternary CIGS target were described in Ref [12]. In order to improve the efficiency, we adopted several modifications for the fabrication of the CIGS absorber layer. First, a bilayer precursor of $(In,Ga)_2Se_3$/CuSe (the two-target process), instead of the single-layered Cu-In-Ga-Se precursor (the single-target process) sputtered from a quaternary CIGS chalcogenide target, were sequentially sputtered on Mo-coated soda-lime glass at room temperature from $(In,Ga)_2Se_3$ and CuSe targets, using high-purity argon discharged with RF sputtering powers of 130 W

* Corresponding authors at: CAS Key Laboratory of Materials for Energy Conversion, Shanghai Institute of Ceramics, Chinese Academy of Sciences, 1295 Dingxi Road, Shanghai 200050, China.
Tel.: +86 21 5241 1620; fax: +86 21 5241 6360.
E-mail address: huangfq@mail.sic.ac.cn (F.Q. Huang).

0927-0248/$ - see front matter © 2013 Elsevier B.V. All rights reserved.
http://dx.doi.org/10.1016/j.solmat.2013.02.001

and 50 W, respectively. Second, the selenization process was implemented in the annealing system consisting of a sample holder and several distributors for solid Se pellets in a graphite box. The CIGS precursors were selenized at 550 °C for 30 min. In the case of the bilayer precursor, the temperature was ramped to 550 °C in 5 min at room temperature.

The fabrication procedure of the CIGS solar cells in the new process was similar to the reported process. Solar cells with glass/Mo/CIGS/CdS/i-ZnO/ZnO:Al/Ag grids structures were fabricated. The CdS buffer layers with a nominal thickness of 50 nm were deposited by chemical bath deposition (CBD). The window layers consisted of a 70 nm-thick i-ZnO and a 800 nm-thick ZnO:Al layer, and both layers were deposited by RF magnetron sputtering. The active sizes of the cells were 0.4 cm^2. No antireflective coatings were employed.

The surface morphologies of as-sputtered and annealed films were examined by SEM and FESEM with a SEM JEOL-6510 and a FEI Magellan 400, respectively. The crystallographic orientations of these films were determined by XRD using a Bruker D8 X-ray diffractometer with Cu Kα irradiation of 40 kV and 40 mA. Finally, the photovoltaic (PV) performance parameters of solar cells based on the grown CIGS layers were measured under a simulated illumination (Solar simulator: Newport Oriel 93194A) with a light intensity of 100 mW/cm^2.

3. Results and discussion

The $(In,Ga)_2Se_3$/CuSe bilayer precursor was sequentially sputtered on Mo-coated soda-lime glass from $(In,Ga)_2Se_3$ and CuSe targets, which resulted in the final CIGS absorber film after annealing in a Se vapor. The precursor structure of CIGS can drastically affect the eventual device performance [13,14]. Therefore, it is vital to characterize the microstructures and physical properties of $(In,Ga)_2Se_3$, $(In,Ga)_2Se_3$/CuSe and Cu-In-Ga-Se precursors, respectively. The XRD patterns of these precursors and as-annealed films are shown in Figs. 1 and 2. The CIGS precursor layer from the single-target process was amorphous (Fig. 1a). However, though the first layer of $(In,Ga)_2Se_3$ was apparently amorphous (Fig. 2a), the $(In,Ga)_2Se_3$/CuSe precursor from the two-target process contained a crystalline α-CuSe phase (Fig. 2b). After these two precursor layers were subject to an annealing treatment in Se vapor, the XRD spectra exhibited no secondary phase, resulting in the formation of a single-phase chalcopyrite-type CIGS structures (Fig. 1b and c). The intensity ratio R of the (220/204) reflection peak and the (112) reflection peak is used to index the texture of the CIGS film. The ratio R is 2.5 in the XRD pattern from JCPDS 35–1102. The corresponding ratios of the single-target and two-target CIGS films were about 3.20 and 2.55, respectively. Therefore, the single-target film revealed a (112) preferred orientation, while the two-target film had a nearly random orientation. The full-width half-maximum (FWHM) value of (112) peak of the annealed two-target CIGS film was around 0.21°, while the single-target CIGS film had a value of about 0.26°. It indicated a better crystallinity for the two-target process CIGS film.

Scanning electron micrographs of planar views from precursors and annealed films from the two-target and single-target processes are shown in Fig. 3. The plate-like crystals were clearly observed on the two-target $(In,Ga)_2Se_3$/CuSe precursor layer (Fig. 3a), which was consistent with the presentation of the α-CuSe phase from the XRD analysis. Nevertheless, the single-target precursor layer did not show a regular crystal shape (Fig. 3c). After annealing, significantly different morphologies of the two samples were observed. The two-target film shows a smoother surface and more compact microstructure in Fig. 3b and d.

The reaction pathway of $(In,Ga)_2Se_3$/CuSe via the In and Cu in conjunction with Cu_xSe and In_xSe was identified to be energetically favorable [15]. In the two-target process, the $(In,Ga)_2Se_3$ layer was amorphous and the CuSe layer contained α-CuSe nanocrystals on the top layer of the precursor. Therefore, the resulting precursor from the two-target process was exceptionally well suited from a thermodynamic point of view to allow for an energetically favorable reaction pathway. Furthermore, it had been reported that the formation of CIGS for the precursor structure of the two-target process occurred at the interface of the CuSe and $(In,Ga)_2Se_3$, following the one-dimensional diffusion [13]. Apparently, this grain growth model was more favor to obtain larger grain size than that of the single-target precursor film, where Cu, In,Ga, and Se were distributed homogeneously. Thus, the grain growth was more apt to follow the Ostwald model, although the detailed reaction pathway had not been reported.

In addition, one of the other possibilities was the beneficial effects of Cuse phases for the growth of chalcopyrite thin films, which generally was regarded to become liquid phase during the growth of CIGS film to aid the formation of the large grains and smooth surface for CIGS film [16]. In the two-target process, these beneficial effects were accomplished by depositing a CuSe layer on top of the precursor and selenizing the precursors in a relatively rapid thermal process. Accordingly, we attributed the improvement in structural quality to both the one-dimensional diffusion growth model and the CuSe-assist grain growth.

The photovoltaic parameters of a 13.6% device (Fig. 4a) revealed a significant improvement of open circuit voltage (V_{oc}),

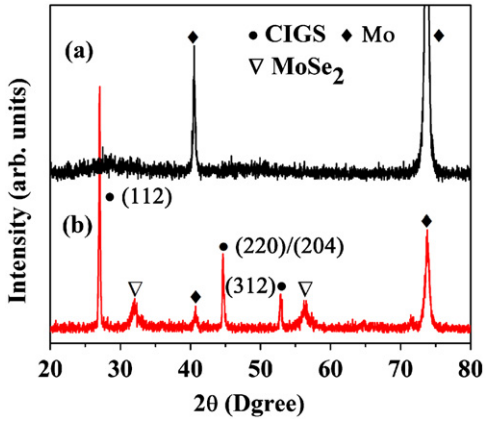

Fig. 1. XRD patterns of (a) CIGS precursor layer sputtered from a single CIGS target and (b) annealed CIGS layer on Mo-coated glass substrates.

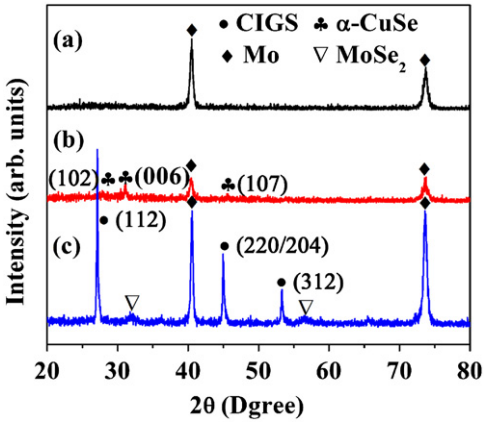

Fig. 2. XRD patterns of (a) $(In,Ga)_2Se_3$, (b) $(In,Ga)_2Se_3$/CuSe, and (c) annealed $(In,Ga)_2Se_3$/CuSe layers on Mo-coated glass substrates.